

First *XMM-Newton* observations of strongly magnetic cataclysmic variables I: spectral studies of DP Leo and WW Hor

Gavin Ramsay¹, Mark Cropper¹, France Córdova², Keith Mason¹, Rudi Much³, Dirk Pandel², Robert Shirey²

¹*Mullard Space Science Lab, University College London, Holmbury St. Mary, Dorking, Surrey, RH5 6NT, UK*

²*Department of Physics, University of California, Santa Barbara, California 93106, USA*

³*Astrophysics Division, ESTEC, 2200, AG Noordwijk, The Netherlands*

Received:

ABSTRACT

We present an analysis of the X-ray spectra of two strongly magnetic cataclysmic variables, DP Leo and WW Hor, made using *XMM-Newton*. Both systems were in intermediate levels of accretion. Hard optically thin X-ray emission from the shocked accreting gas was detected from both systems, while a soft blackbody X-ray component from the heated surface was detected only in DP Leo. We suggest that the lack of a soft X-ray component in WW Hor is due to the fact that the accretion area is larger than in previous observations with a resulting lower temperature for the re-processed hard X-rays. Using a multi-temperature model of the post-shock flow, we estimate that the white dwarf in both systems has a mass greater than $1 M_{\odot}$. The implications of this result are discussed. We demonstrate that the ‘soft X-ray excess’ observed in many magnetic cataclysmic variables can be partially attributed to using an inappropriate model for the hard X-ray emission.

Key words: Stars: binaries: eclipsing – Stars: magnetic field – Stars: novae, cataclysmic variables – Stars: individual: DP Leo, WW Hor – X-rays: stars

1 INTRODUCTION

Polars, or AM Her systems, are interacting binary systems in which the magnetic field of the accreting white dwarf is strong enough to prevent the formation of an accretion disc. It also forces the spin period of the white dwarf to be synchronised with the binary orbital period. In these systems, the accreting material leaves the red dwarf secondary, follows a ballistic trajectory before getting coupled by the magnetic field of the white dwarf and funnelled directly onto the white dwarf surface.

Just above the white dwarf photosphere, the accretion flow is strongly shocked, at which point the temperature reaches $\sim 50\text{keV}$. Some of this radiation is intercepted by the white dwarf where it is thermalised and re-radiated as soft X-rays. An additional source of soft X-rays is dense blobs of material which penetrate into the white dwarf photosphere and heat it directly. In addition, there is a cyclotron component which is strongest in the optical band (for the magnetic field strength found in polars: $\sim 10\text{--}200\text{MG}$). This arises from electrons spiralling around the magnetic field lines close to the shock.

Prior to the launch of the *ROSAT* X-ray satellite in

1990 the relative strength of the three emission components was a major issue (eg King & Watson 1987). Observations of several polars showed that the strength of the soft X-ray component relative to the hard X-ray component was in excess of that predicted by simple accretion models (eg Heise et al 1985). With the results derived using *ROSAT* it became clear that many polars showed this ‘soft X-ray excess’ (Ramsay et al. 1994). During epochs when the accretion rate was in an ‘intermediate’ level of accretion, Ramsay, Cropper & Mason (1995) found that the relative strength of the soft X-ray flux was less than in ‘high’ accretion states: indeed AM Her showed a ‘soft X-ray deficiency’ in this state. They hypothesized that for lower accretion rates, a shock does not form over the whole of the accretion region.

A significant uncertainty in the results of Ramsay et al (1994) was the poor constraint on the hard X-ray flux since *ROSAT* did not extend to energies much higher than $\sim 2\text{keV}$. With the launch of *XMM-Newton* we are able, for the first time, to detect both the soft and hard X-ray components clearly. This paper presents an analysis of the spectra of the first polars to be observed using *XMM-Newton*.

Object	Observation Date	Effective exposure (ksec) PN, MOS
DP Leo	22 Nov 2000	19, 18
WW Hor	4 Dec 2000	21, 23

Table 1. The observation log of the *XMM-Newton* observations of DP Leo and WW Hor. In the case of the DP Leo observations, time intervals of enhanced particle background were excluded.

EPIC detector	response file used
PN	epn_fs20_Y9_thin.rmf
MOS1	m1_thin1v9q19t5r4_all_15.rsp
MOS2	m2_thin1v9q19t5r4_all_15.rsp

Table 2. The response files used in the analysis.

2 OBSERVATIONS

DP Leo and WW Hor were observed using *XMM-Newton* in Nov and Dec 2000 respectively: the observation log is shown in Table 1. Both objects were detected in all three EPIC detectors (Turner et al 2001, Stüder et al 2001), which were configured in full window mode and used the thin filter. Neither object was detected in the RGS detectors. During the DP Leo observations, there were time intervals of enhanced particle background. These intervals were removed from the spectral analysis, reducing the exposure by 16ksec in the EPIC detectors. The observations of WW Hor were not significantly effected by increased particle background. By comparing the X-ray and optical flux with previous observations, it was concluded that both systems were in an intermediate state of accretion (cf Pandel et al 2001).

Before extracting source spectra, the data were processed using the first public release of the *XMM-Newton* Science Analysis System. Spectra were extracted from the EPIC PN camera data using an aperture of $\sim 19''$ in radius centered on the source, chosen so that the aperture did not cover more than one CCD. This encompasses ~ 85 percent of the integrated PSF (Aschenbach et al 2000). In the case of the EPIC MOS data, the source was in the centre of the CCD and a radius of $\sim 24''$ was used (encompassing ~ 90 percent of the integrated PSF). Background spectra were extracted from the same CCD on which the source was detected, scaled and subtracted from the source spectra.

Since the response of the EPIC PN detector is not well calibrated at present below ~ 0.2 keV, energies below this were ignored in the subsequent analysis. Also the PN response function used assumes only single pixel events, so we extracted only these events to construct our PN spectrum. For the EPIC MOS detectors, which are currently better calibrated at lower energies, we fitted energies above 0.1keV. The response files used in the analysis are listed in Table 2.

3 THE MODEL FOR THE X-RAY SPECTRUM

The hard X-ray component produced in the hot post-shock flow has traditionally been modelled using a single temperature thermal bremsstrahlung component. We have developed a physically more realistic model of the post-shock flow (Wu, Chanmugam & Shaviv 1994, Cropper, Ramsay & Wu

1998), which takes account of its multi-temperature nature and the fact that a significant fraction of the cooling takes place in the form of cyclotron radiation. It also includes the hard X-rays reflected from the surface of the white dwarf. In addition, Cropper et al (1999) included the effect of the varying gravitational force over the height of the post-shock flow. In this paper we use the model of Cropper et al (1999) to model the hard X-ray component and a blackbody to model any soft X-ray component. In addition, we account for absorption using a neutral absorption model.

4 DP LEO

The integrated EPIC PN and MOS1 spectra of DP Leo are shown in Figure 1. A soft X-ray component is seen together with a hard component – this is the first time that DP Leo has been detected above 2keV. Line emission from Fe $K\alpha$ is detected at ~ 6.7 keV.

We fitted all three EPIC X-ray spectra separately using the model described in §3. We fix the specific accretion rate, \dot{m} , at $1 \text{ g s}^{-1} \text{ cm}^{-2}$ (appropriate for a system in an intermediate accretion state), the ratio of cyclotron to bremsstrahlung cooling, ϵ_s , at 10 (appropriate for the magnetic field strength seen in DP Leo: 31MG Cropper & Wickramasinghe 1993) and the metal abundance at solar. The fit is not sensitive to the exact values chosen for these parameters.

The best fit parameters are shown in Table 3: good fits are achieved. The absorption towards DP Leo is low, $< 10^{20} \text{ cm}^{-2}$ and the temperature of the blackbody is similar to that found for other polars (eg Ramsay et al 1994). To determine the implied mass of the white dwarf we assume the Nauenberg (1972) mass-radius relationship for white dwarfs. This yields a white dwarf mass greater than $1.3M_{\odot}$.

We also show in Figure 1, the spectra centered on 7keV. Our model fits underestimate the line flux for the Fe $K\alpha$ emission lines. To investigate this further, we varied the metal abundance, ϵ_s and \dot{m} . No solution was achievable that was consistent with both the line and continuum flux. We address this further in §6.

We show in Table 3 the unabsorbed, bolometric fluxes for the soft and hard X-ray components. The soft X-ray luminosity is defined as $L_{soft,bol} = \pi f_{soft,bol} \sec(i - \beta) d^2$, where we assume that the soft X-ray emission is optically thick and can be approximated by a small thin slab of material, the unabsorbed bolometric blackbody flux is $f_{soft,bol}$, d is the distance, i is the system inclination and β is the angle between the accretion region and the spin axis. For DP Leo, $i = 80^\circ$ and $\beta = 100^\circ$ (Bailey et al 1993), while Biermann et al (1985) find $d > 380 \text{ pc}$. Because we have been able to extend to lower energies in the MOS detectors compared to the PN detector (since they are currently better calibrated), the absorption is more constrained using the MOS detectors. In determining the flux from the soft component using the PN data we have constrained the absorption to be $< 9 \times 10^{19} \text{ cm}^{-2}$ – the upper limit derived from the MOS detectors.

We define the hard X-ray luminosity as $L_{hard,bol} = 4\pi f_{hard,bol} d^2$, where $f_{hard,bol}$ is the unabsorbed, bolometric flux from the hard component. Since a fraction of the hard X-ray flux is directed towards the white dwarf and some of that is reflected back towards the observer, we switch the

reflected component to zero after the final fit to determine the intrinsic flux from the optically thin shocked material.

We also show in Table 3 our estimate of the ratio $L_{soft,bol}/L_{hard,bol}$. Using data obtained using *ROSAT*, Ramsay et al (1994) were able to put an upper limit only on this ratio since the hard X-ray component was not significantly detected. Now using the *XMM-Newton* data, we can place relatively good constraints on the ratio because we sample both the hard and soft X-ray components. If there were no dense blobs of material in the accretion stream, we expect $L_{soft,bol}/L_{hard,bol} \sim 0.5$ (in some polars in a high state of accretion, it is found that this ratio is much greater than this; on the other hand, for systems in intermediate states of accretion, the ratio can be much lower). The $L_{soft,bol}/L_{hard,bol}$ ratio in DP Leo, is around unity, implying consistency with the standard Lamb and Masters (1979) model.

Cropper, Wu & Ramsay (2000) suggest that using a single temperature thermal bremsstrahlung to model the hard X-ray component will contribute to the apparent ‘soft X-ray excess’ seen in many polars. This is because a fraction of the photons attributed to the soft X-ray component actually originates in the lowest levels of the post-shock flow rather than from re-processing by the white dwarf. Our multi-temperature shock model intrinsically emits a significant amount of soft X-rays at the base of the post-shock flow. It is interesting to determine the soft to hard X-ray ratio if we assume an absorbed blackbody plus single temperature thermal bremsstrahlung model as used by Ramsay et al (1994). Fixing the thermal bremsstrahlung temperature at 30keV (as there), and adding a Gaussian to model the Fe K α line emission at ~ 6.7 keV, we find that the ratio, $L_{soft,bol}/L_{hard,bol}$ is twice the value determined using the multi-temperature model. This suggests that when comparing the relative strength of the shocked and re-processed X-ray components, it is essential to use the most physically realistic model of the post-shock flow available.

5 WW HOR

The integrated EPIC PN and MOS1 spectra of WW Hor are shown in Figure 2. Whilst we observe hard X-ray emission above 2keV in WW Hor for the first time, there is no evidence for a soft blackbody component with the sort of temperature seen in DP Leo. This is unusual, since even for systems in a reduced rate of accretion a soft X-ray component is expected. Weak Fe K α line emission is present at 6.7 keV. In the PN spectrum there is evidence for an emission line due to Fe fluorescence near 6.4keV.

We modelled the integrated EPIC spectra from each detector separately using the model described in §3 together with a neutral absorber. As in DP Leo we fix \dot{m} , at $1 \text{ g s}^{-1} \text{ cm}^{-2}$, ϵ_s at 10 and the metal abundance at solar. We obtain good fits: the best fit model parameters are shown in Table 3. We find a very low absorption column. The mass of the white dwarf is $\sim 1.1M_{\odot}$. Using a distance of 430pc (Bailey et al 1988) we estimate the unabsorbed, hard bolometric luminosity to be $L_{hard} = 1 - 2 \times 10^{31} \text{ ergs s}^{-1}$. This is similar to that found for other AM Her systems in intermediate accretion states (Ramsay, Cropper & Mason 1995). Indeed, when we compare the phase averaged observed flux

in the 0.1–2.0keV band in *XMM-Newton* ($2.1 \times 10^{-13} \text{ ergs s}^{-1} \text{ cm}^{-2}$ in MOS1) with the *ROSAT* observation of WW Hor, made when it was in an intermediate state ($2.3 \times 10^{-13} \text{ ergs s}^{-1} \text{ cm}^{-2}$), we find that they are very similar.

We can investigate whether a low temperature soft X-ray component could be absorbed by a modest absorption column. In the lowest energy bands the best calibrated instrument is the EPIC MOS1 detector. We added a blackbody component with temperature $kT_{bb}=10$ and 15 eV to the model used above (cf $kT_{bb} \sim 30$ eV for DP Leo). We find that such a low temperature blackbody is ‘hidden’ by an absorption column consistent with our upper limit ($5.6 \times 10^{19} \text{ cm}^{-2}$). The corresponding values of L_{soft} is 8.5×10^{30} and $4.3 \times 10^{30} \text{ ergs s}^{-1}$ for 10 and 15eV respectively. This corresponds to $L_{soft}/L_{hard}=0.4$ and 0.2: these values are broadly similar to that found for polars in intermediate accretion states (Ramsay, Cropper & Mason 1995).

6 DISCUSSION

When WW Hor was observed using *ROSAT* it was found that both a blackbody and a bremsstrahlung component were required to fit the X-ray spectrum (Ramsay, Cropper & Mason 1995). When WW Hor was observed using *XMM-Newton*, it was at very similar X-ray flux levels compared to the *ROSAT* observation. Further, the X-ray bolometric luminosity of WW Hor is approximately similar to DP Leo (implying similar mass transfer rates) if we assume similar distances. Why do we therefore observe a soft X-ray component in DP Leo and not WW Hor?

We suggest that the accretion region was more spread out in the *XMM-Newton* observation of WW Hor compared to the *ROSAT* observation, thereby decreasing the local heating rate and causing the temperature of any soft X-ray component to decrease. If it was sufficiently low (say $kT=10$ or 15eV), we showed in §5 that even a very modest amount of absorption would prevent us from detecting this soft X-ray component. It is not clear why the accretion region would cover a larger area of the white dwarf. One possible reason could be that for relatively low mass transfer rates, accretion occurs onto a wide range of magnetic azimuths, resulting in a more extended accretion region. This is thought to be one of the reasons why intermediate polars (which have less strong magnetic fields than polars) do not show a soft X-ray component (eg King & Lasota 1990).

We now briefly comment on the derived masses for the white dwarfs in these systems. In the case of WW Hor, we find a mass of $\sim 1.1M_{\odot}$ and for DP Leo $>1.3M_{\odot}$ (table 3). The mass of the white dwarf in both systems is at the upper end of expectations. There are no other accurate estimates for the mass of the white dwarf in these two systems. Several magnetic CVs were found to have similar masses to WW Hor in the survey of such systems using *RXTE* data and the same emission model as used here (Ramsay 2000). Similarly, the mass of Sirius B is 1.034 ± 0.026 (Holberg et al 1998). Other massive non-accreting white dwarfs have been found (eg RE J0317–858; $1.31\text{--}1.37M_{\odot}$, Ferrario et al 1997). In the case of DP Leo, however, the mass of the white dwarf is very heavy indeed and would be the heaviest white dwarf within an accreting magnetic system yet found. Ramsay (2000) found that the mass distribution of isolated non-magnetic white

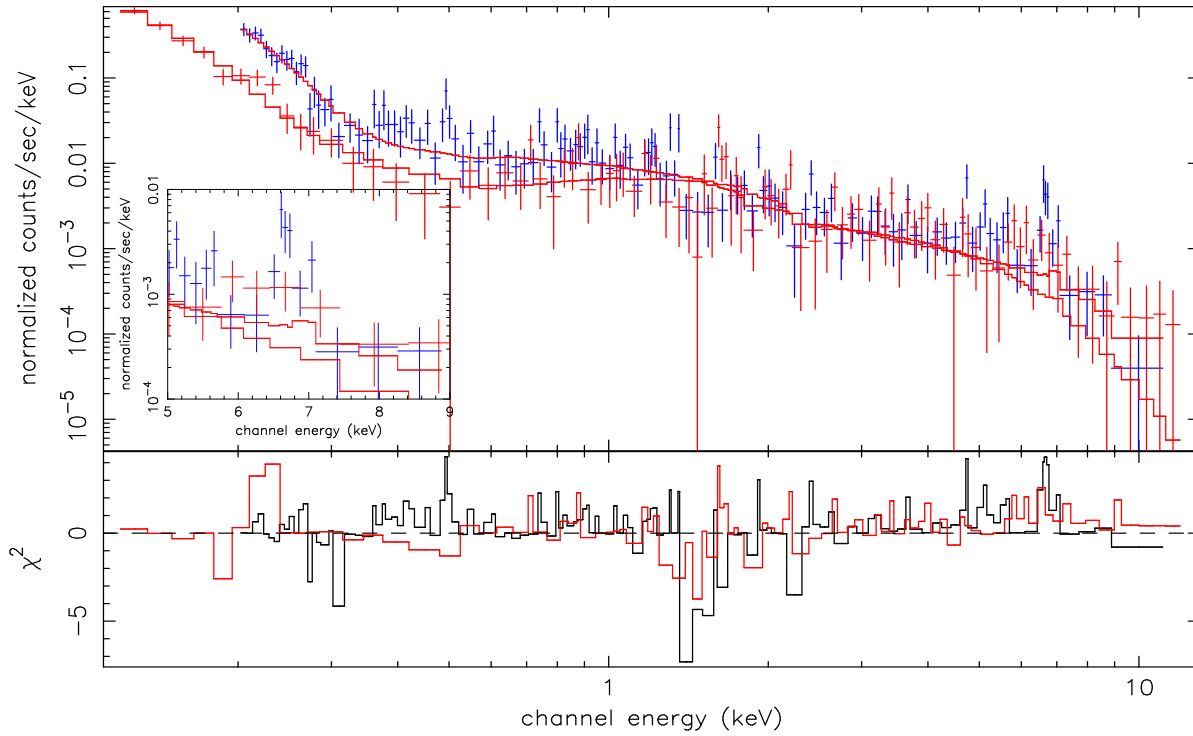


Figure 1. The EPIC PN (upper), MOS1 (lower) X-ray spectra of DP Leo. The solid lines show the best fit using an absorbed blackbody plus multi-temperature accretion shock model.

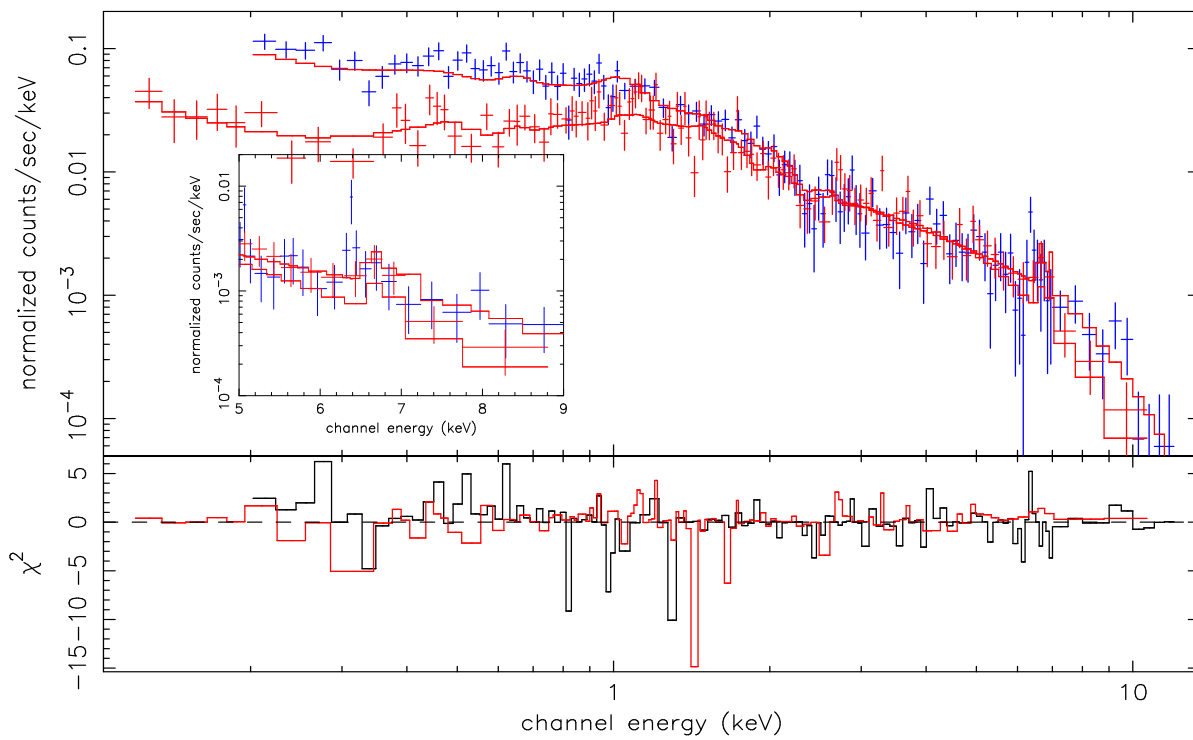


Figure 2. As for figure 1, but for WW Hor

		N_H ($\times 10^{19}$ cm^{-2})	kT_{bb} (eV)	M_1 (M_\odot)	Flux $_{soft,bol}$ ($\times 10^{-12}$ erg $\text{s}^{-1} \text{cm}^{-2}$)	$L_{soft,bol}$ ($\times 10^{31}$ ergs s^{-1})	Flux $_{hard,bol}$ ($\times 10^{-13}$ erg $\text{s}^{-1} \text{cm}^{-2}$)	$L_{hard,bol}$ ($\times 10^{31}$ ergs s^{-1})	$L_{soft,bol}/$ $L_{hard,bol}$	χ^2_ν (dof)
DP Leo	PN	0.0 ⁺²⁰	23 ⁺⁴ ₋₅	1.40 _{-0.12}	6.7 ^{+36.2} _{-3.7}	3.4 ^{+18.6} _{-1.4}	4.4 ^{+0.8} _{-0.5}	0.8 ^{+0.1} _{-0.1}	4.2 ⁺²⁹ _{-3.0}	1.12 (126)
	MOS1	2.1 ^{+6.9} _{-0.6}	30 ⁺³ ₋₆	1.40 _{-0.09}	2.5 ^{+9.5} _{-0.8}	1.3 ^{+4.9} _{-0.5}	6.6 ^{+1.0} _{-1.0}	1.3 ^{+0.1} _{-0.2}	1.0 ^{+5.7} _{-0.5}	0.88 (90)
	MOS2	3.3 ^{+5.7} _{-1.8}	28 ⁺³ ₋₅	1.40 _{-0.08}	3.3 ^{+3.7} _{-1.5}	1.6 ^{+2.0} _{-0.7}	6.6 ^{+1.3} _{-0.9}	1.3 ^{+0.2} _{-0.1}	1.2 ^{+2.4} _{-0.8}	1.05 (72)
WW Hor	PN	0.0 ^{+1.4}		1.04 ^{+0.05} _{-0.06}			7.6 ^{+0.4} _{-0.3}	1.7 ^{+0.1} _{-0.1}		1.25 (123)
	MOS1	1.4 ^{+4.2} _{-1.2}		1.18 ^{+0.10} _{-0.09}			12.8 ^{+1.0} _{-1.5}	2.8 ^{+0.2} _{-0.2}		1.02 (116)
	MOS2	0.0 ^{+1.6}		0.99 ^{+0.06} _{-0.05}			7.6 ^{+0.4} _{-0.5}	1.7 ^{+0.1} _{-0.1}		0.98 (165)

Table 3. The best fit parameters to the EPIC PN, MOS1 and MOS2 data of DP Leo and WW Hor using the multi-temperature model described in §3. A distance of 400pc is assumed for DP Leo (Biermann et al 1985 find $d > 380\text{pc}$) and 430pc for WW Hor (Bailey et al 1998). In determining the fluxes and luminosities of DP Leo using the PN data, we have chosen an upper limit of $N_H < 9 \times 10^{19} \text{cm}^{-2}$ which is the upper limit derived from the MOS data (which has a better response at lower energies).

dwarfs and white dwarfs in magnetic CVs are significantly different: the white dwarfs in magnetic CVs are biased towards heavier masses. However, it was not clear if this was due to selection effects: it is possible that high mass polars are more likely to be discovered than low mass polars.

In calculating the mass of the white dwarf we use the Nauenberg (1972) approximation for the white dwarf mass-radius relationship: this approximates the Hamada & Salpeter (1961) mass-radius relationship for carbon white dwarfs over the range 0.3–1.2 M_\odot , and is consistent with the best mass-radius data for the white dwarfs 40 EriB and Sirius B (Provencal et al 1988). However the appropriate mass-radius relationship is still a matter of debate. In the case of DP Leo, where we estimate a white dwarf of mass $> 1.3M_\odot$, there is some additional uncertainty for our mass estimate since for the very heaviest white dwarfs the mass-radius relationship is very uncertain. Hamada & Salpeter (1961) also show the mass-radius relationship for Fe core white dwarfs. White dwarfs with Fe cores are thought to be formed when a white dwarf with a ONeMg core ignites through an accretion-driven collapse (Isern, Canal & Labay 1991). The maximum mass for such a white dwarf is $\sim 1.1M_\odot$. Using this mass-radius relationship we obtain a mass of $\sim 1.1M_\odot$, again close to the maximum.

Alternatively, it is possible that additional cooling processes not included in our model could become important for white dwarfs greater than $1.0M_\odot$. This would have the effect of modifying the temperature-height profile of the post-shock region and hence the implied X-ray spectrum. If the volume of gas emitting $\lesssim 10\text{keV}$ was underestimated, then this may also account for the deficit of Fe line emission in DP Leo (§4). In general, however, additional cooling terms work to soften the X-ray spectrum, resulting in a higher gravitational potential (and hence white dwarf mass) to fit the observed spectrum. It is also possible that the absorption is more complex than a simple neutral absorber, as was found to be the case in the polar BY Cam (Done & Magdziarz 1998). This would make the continuum appear harder, so overestimating the shock temperature and hence the white dwarf mass. The higher temperature continuum would also underpredict the plasma iron lines fluxes. Given that both these features are seen in our model fits, we added a partial covering component and also an ionized absorption component to our model. The resulting fits and masses were not significantly improved with the exception of the MOS1 data which gave masses which were 0.1–0.2 M_\odot lighter. Data of

higher signal to noise would be required to test the necessity of more complex absorption models.

7 ACKNOWLEDGEMENTS

Based on observations obtained with XMM-Newton, an ESA science mission with instruments and contributions directly funded by ESA Member States and the USA (NASA).

REFERENCES

- Aschenbach, B., et al, 2000, SPIE 4012, paper 86
 Bailey, J., Wickramasinghe, D. T., Hough, J. H., Cropper, M., 1988, MNRAS, 234, 19P
 Bailey, J., Wickramasinghe, D. T., Ferrario, L., Hough, J. H., Cropper, M., 1993, MNRAS, 261, L31
 Biermann, P., et al 1985, ApJ, 293, 303
 Cropper, M. & Wickramasinghe, D. T., 1993, MNRAS, 260, 696
 Cropper, M., Ramsay, G., Wu, K., 1998, MNRAS, 293, 222
 Cropper, M., Wu, K., Ramsay, G., Kocabiyyik, A., 1999, MNRAS, 306, 684
 Cropper, M., Wu, K., Ramsay, G., 2000, New Astrn Rev, 44, 57
 Done, C., Magdziarz, P., 1998, MNRAS, 298, 737
 Ferrario, L., Vennes, S., Wickramasinghe, D. T., Bailey, J., Christian, D. J., 1997, MNRAS, 292, 205
 Hamada, T., Salpeter, E. E., 1961, ApJ, 134, 683
 Heise, J., Brinkman, A. C., Gronenschild, E., Watson, M. G., King, A. R., Stella, L., Kieboom, K., 1985, A&A, 148, L14
 Holberg, J. B., Barstow, M. A., Bruhweiler, F. C., Cruise, C. M., Penny, A. J., 1998, ApJ, 497, 935
 Isern, J., Canal, R., Labay, J., 1991, ApJ, 372, L83
 King, A. R., Watson, M. G., 1987, MNRAS, 227, 205
 King, A. R., Lasota, J. P., 1990, MNRAS, 247, 214
 Lamb, D. Q., Masters, A. R., 1979, ApJ, 234, L117
 Nauenberg, M., 1972, ApJ, 175, 417
 Pandel, D., et al, in prep
 Provencal, J. L., Shipman, H. L., G, E. H., Thejll, P., 1998, ApJ, 494, 759
 Ramsay, G., Mason, K. O., Cropper, M., Watson, M. G., Clayton, K. L., 1994, MNRAS, 270, 692
 Ramsay, G., Cropper, M., Mason, K. O., 1995, MNRAS, 276, 1382
 Ramsay, 2000, MNRAS, 314, 403
 Stüder, L., 2001, 365, L18
 Turner, M., et al 2001, A&A, 365, L27
 Wu, K., Chanmugam, G., Shaviv, G., 1994, ApJ, 426, 664